Research Article

Journal of RAMAN SPECTROSCOPY

Received: 31 August 2008 Accepted: 4 December 2008 Published online in Wiley Interscience: 23 February 2009

(www.interscience.wiley.com) DOI 10.1002/jrs.2185

In situ monitoring of solid-state transition of *p*-aminobenzoic acid polymorphs using Raman spectroscopy

Xia Yang, Xiujuan Wang* and Chi Bun Ching

The purpose of this study is to investigate the mechanism of solid-state polymorphic transition of *p*-aminobenzoic acid (PABA) using *in situ* Raman spectroscopy measurement. The polymorphic transition experiments were conducted on a micro quartz vessel mounted on a microscope, hot and cold stage, under isothermal conditions. The temperature was precisely controlled by a standalone temperature controller equipped with liquid nitrogen cooling system. The Raman spectroscopy probe was positioned on the surface of the solid sample in the micro vessel. The polymorphic transition progression was *in situ* monitored and recorded by Raman spectroscopy. Based on the polymorphic transition rate resulted from the quantitative analysis of Raman spectra, the mechanism of solid-state polymorphic transition of PABA was examined by various empirical kinetic models. An Arrhenius analysis was also performed to calculate activation energies from 134.7 kJ mol^{-1} to 137.7 kJ mol^{-1} for the transition. The results demonstrated that *in situ* Raman spectroscopy is a valuable and accurate technique to probe polymorphic transition process. Copyright © 2009 John Wiley & Sons, Ltd.

Keywords: polymorph; *in situ* Raman spectroscopy; solid-state transition; kinetics; *p*-aminobenzoic acid

Introduction

Polymorphism is the ability of a chemical compound to exist in more than one crystalline form. Each form has the same chemical structure but different arrangements of molecules in the crystal lattice.[1,2] This phenomenon is frequently observed in organic materials where different polymorphs of the same compound may exhibit significantly different chemical and physical properties. Polymorphism and its occurrence have become important issues in current pharmaceutical and fine chemical research and development.

From thermodynamic consideration, only one polymorph is stable at a specific temperature and pressure, and a metastable polymorph will theoretically transform to a more stable form. The transformation between polymorphs involves both thermodynamic and kinetic control. Polymorphic transformation from a less stable form to a more stable form is predicted to be spontaneous and inevitable, but the transformation process may last for seconds, days or even millennia depending on the environmental conditions (temperature, pressure, solvent, etc.). Polymorphic transformation proceeds generally via solution-mediated transformation and solid-state transition. Solution-mediated transformation occurs in the presence of a solvent via dissolution of a less stable form and nucleation of a more stable form. The thermodynamic driving force for the polymorphic transformation is the difference of free energy, specifically the solubility difference between the two polymorphs.[3,4] Solid-state transition is believed to result from the molecular reorientation in the crystal lattice of metastable form.[5] The solid-state transition takes place without passing through liquid or vapor media and its occurrence is much influenced by kinetic parameters.

The solid-state stability of biomolecules and pharmaceutical products is a critical issue in the chemical and pharmaceutical industry. As for a compound having more than one polymorph, the solid-state transition between different polymorphs can have significant effects on its physical and chemical properties, and eventually modify the pharmaceutical properties, such as solubility, dissolution, and bioavailability. As a result, kinetic study of solid-state polymorphic transition under various operating conditions is of particular importance.

The kinetic study of a polymorphic transition involves characterizing, monitoring, and modeling the transition process. The conventional analytical techniques frequently used for characterizing transition processes are powder X-ray diffraction (PXRD),[6] differential scanning calorimetry (DSC),[7] and Fourier transform infrared spectroscopy (FTIR).[8,9] These off-line techniques, however, usually require sample isolation and invasive preparation before the measurements, which may introduce error into the measured kinetic parameters. Recently, Raman spectroscopy has been successfully applied to identify different polymorphic forms and monitor the polymorphic crystallization.[10,11] Many research groups have reported the application of *in situ* Raman spectroscopy to characterize solution-mediated transformation, including study of L-glutamic acid,[12,13] glycine,[14] carbamazepine[15,16] and References. [17–19] These publications show that Raman spectroscopy is a simple, rapid, and reliable real-time technique for probing the polymorphic transformation in solution. However, not many attempts have been conducted in regard to monitoring solid-state transition using Raman spectroscopy, especially to obtaining kinetic information under *in situ* conditions.

* *Correspondence to: Xiujuan Wang, School of Chemical and Biomedical Engineering, Nanyang Technological University, N1.2-B3-08, 62 Nanyang Drive, Singapore 637459 Singapore. E-mail: wangxj@ntu.edu.sg*

School of Chemical and Biomedical Engineering, Nanyang Technological University, N1.2-B3-08, 62 Nanyang Drive, Singapore 637459, Singapore

Journal of RAMAN SPECTROSCOPY

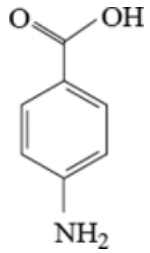

Figure 1. Chemical structure of *p*-Aminobenzoic acid.

The model compound in this study is *p*-aminobenzoic acid (PABA), which is an essential nutrient for several micro-organisms and it is an important active ingredient in the manufacture of sunscreens, esters, folic acid.[20,21] PABA, as shown in Fig. 1 for chemical structure, is known to have two polymorphs identified as α-form ($a = 18.551$ Å, $b = 3.860$ Å, $c = 18.642$ Å, $Z = 8$, space group $P2_1/n$)[22] and β-form ($a = 6.275$ Å, $b = 8.55$ Å, $c = 12.80$ Å, $Z = 4$, space group $P2_1/c$).[23] The needle-shaped α-form is commercially available. It has been reported that the polymorphs α and β of PABA exhibit an enantiotropic behavior, in which the β-form undergoes an endothermic solid–solid transition to the α-form below the melting point.[24] In this study, we report *in situ* measurements of solid-state isothermal transition from β-form PABA to α-form by means of Raman spectroscopy. The two polymorphs were identified and characterized using PXRD and thermogravimetric analysis-differential scanning calorimetry (TGA-DSC). The isothermal solid-state transitions were carried out at different temperatures to extract kinetic information for the transition. Various solid-state kinetic models have been applied to examine the temperature-dependent transition and to determine the activation energy. The results suggest that the *in situ* Raman spectroscopic monitoring and collecting technique is a powerful tool to reveal the solid-state polymorphic transition progression and mechanism.

Experimental

Materials

The α-form PABA was purchased from Sigma-Aldrich and used as received. The β-form was prepared by a solution-mediated transformation of the α-form in aqueous solution. The ultra pure deionized water was obtained through a Millipore ultrapure water system (Milli-Q Gradient A10 System).

Apparatus

PXRD was performed on a Bruker D8 Advance diffractometer. The powders were packed tightly in the sample holder with a 2-mm indent. Each sample was exposed to Cu-Kα radiation at 40 mA and 40 kV. The scanning region of the diffraction angle (2θ) was between 5 and 40° with a step size of 0.05° and scanning speed of 5° min^{-1}.

The thermal behavior of the samples was investigated using thermogravimetric analysis (TGA) and DSC characterization. TGA was performed with a Thermal TA instrument, SDT Q600, at a heating rate of 10 °C min^{-1} under nitrogen flux. DSC measurements were carried out using a Mettler Toledo DSC 822e together with the STARe–software. Samples of 5–7 mg were heated at the increasing temperature rate of 10 °C min^{-1} with purging nitrogen.

The solid-state polymorphic transition of the β-form of PABA to α-form was performed at different temperatures under ambient environment. The experiments were carried out on a Linkam hot and cold microscope stage (Linkam THMS 600, UK) accommodating a micro quartz cell (15 mm diameter × 2 mm depth). Approximately 80 mg of powder sample was compressed to form a 13-mm diameter disk in an evacuated die at 3.5 tons for 1 min. The disk was placed in the quartz cell mounted on the hot stage which had been preheated to the desired temperature. Raman spectra were collected *in situ* from the sample via an immersion fiber-optic probe (305 mm length × 12.7 mm diameter) attached to the 785-nm RamanRXN1 analyzer from Kaiser Optical Systems, Inc. (KOSI, USA). The Raman spectra were collected at an interval of 0.1–5 min. Each spectrum was the accumulation of 2 scans and the exposure time for each scan was 10 seconds. The obtained Raman spectra were processed using HoloGRAMS software package from KOSI.

Results and Discussion

Solid characterization of PABA forms α and β

The PXRD patterns of the α-form and the prepared β-form of PABA over the range of $2\theta = 5$ to 40° are presented in Fig. 2. The characteristic peak of the α-form is observed at 15.36° and the peak at 27.88° is characteristic for the β-form.

The thermal analysis of α-form and β-form of PABA were conducted using TGA and DSC. In order to remove the effect of different particle size on the thermograms,[24] our experimental samples were prepared by grinding α-form and β-form crystals and separating them using an L3P Sonic sifter with 75-mm diameter sieves. The sample was collected from sieve aperture between 20 µm and 25 µm. Figure 3 shows TGA-DSC thermograms for the α-form and β-form at a heating rate of 10 °C min^{-1}. For the α-form, there is no significant weight loss before 180 °C and a steady decrease in weight is observed up to 290 °C. The DSC trace exhibits a sharp melting endothermic peak with an onset of 190 °C, which eliminate the possibility of phase transition from α-form to other polymorphs. Next, another partially resolved endothermic peak is observed at 245 °C due to the decomposition of the compound. The DSC trace of form β is quite similar to that observed for the α-form except that there is a small endothermic peak at 95 °C. Two major endothermic peaks around 189 and 243 °C are observed attributed to melting and decomposition of the compound, respectively. No significant weight loss can be observed for the β-form until the melting point is reached. It has been reported that the β-form undergoes an endothermic solid–solid transition to the α-form below the melting point.[24] In order to confirm that the DSC peak at 95 °C is due to the transition of form β, the β-form crystals have been heated up to 100 °C at 10 °C min^{-1} and then cooled back to room temperature at 20 °C min^{-1}. The PXRD pattern of the sample after the heating–cooling circle was found to present the same feature of form α. The results of thermal analysis for forms α and β of PABA state that the two forms are related enantiotropically.

Figure 4(A) shows the Raman spectra of the forms α and β in the range of 200–3100 cm^{-1}. Some distinct differences can be discerned between the two forms. One of the major differences is the strong band at 1695 cm^{-1} corresponding to the C=O stretching mode of carboxylic acid groups for the β-form. The absence of the C=O stretching mode of α-form in this wavenumber region may be interpreted in terms of the changes in hydrogen bonding. As it was previously reported,[24] the α- and

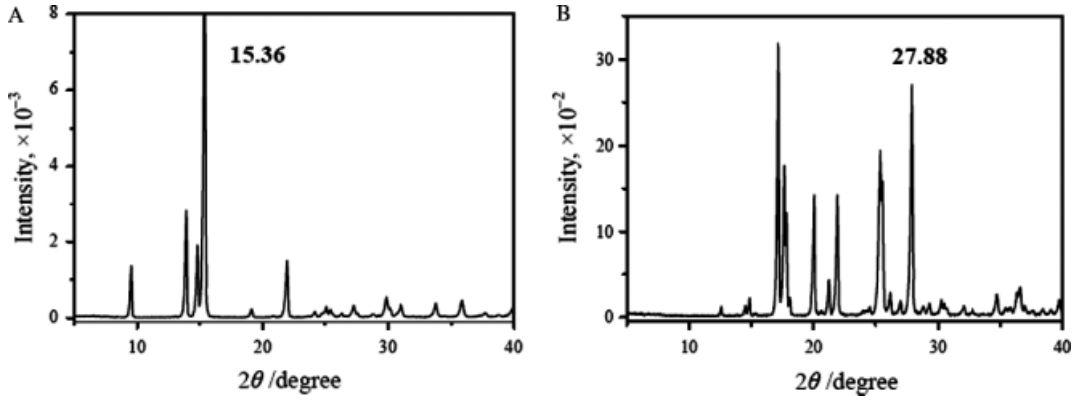

Figure 2. Powder X-ray diffraction patterns of PABA polymorphs: (A) α-form and (B) β-form.

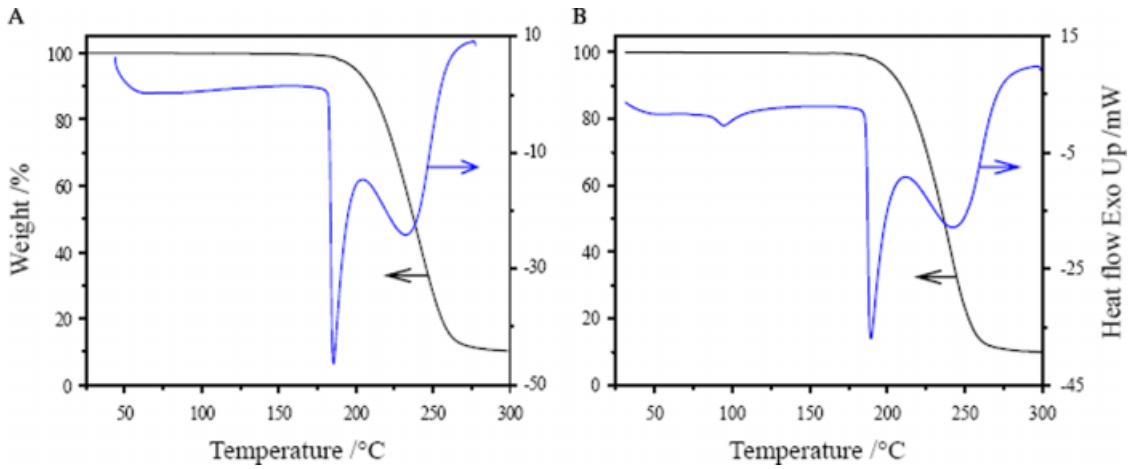

Figure 3. Combined TGA and DSC traces of PABA: (A) α-form and (B) β-form. This figure is available in colour online at www.interscience.wiley.com/journal/jrs.

β-forms have different molecular packing arrangements in the crystal lattice. The crystal structure of α-form consists of hydrogen-bonded dimers by the association of the carboxylic acid groups. It is possible that the C═O bond is weakened as hydrogen-bonded dimer is formed. While in the crystal structure of β-form, there are no carboxylic acid dimers but four-membered rings of alternating amino groups and carboxylic acid groups. The comparative spectra differences of the two forms are highlighted in the region of 1150–1350 cm^{-1}, as shown in Fig. 4(B). In the α-form there are peaks at 1181, 1286, 1313, and 1434 cm^{-1}, while the peaks at 1167, 1253, 1274, and 1309 cm^{-1} are characteristic for β-form. Therein, the bands associated with C–H in-plane bending at 1181 and 1167 cm^{-1} for α-form and β-form, respectively [inset of Fig. 4(B)], were used to interpret events during the *in situ* monitoring of solid-state polymorphic transition. Table 1 summarizes the main characteristic bands with corresponding assignments by reference to published literatures[25–27] for the α- and β-forms.

Table 1. Selected peak positions in the Raman spectra and assignments for the α-form and β-form of PABA

Approximate assignments	Wavenumber (cm^{-1}) α-form	β-form
γ(C–C–C)	505(vw)	512(vw)
γ(C═O)	616(vw)	615(vw)
β(C–C–C)	640(w)	639(w)
γ(C–H)	846(m)	845(m)
β(C–H)	1181(m)	1167(m)
ν(C–OH)	1286(m)	1274(w)
ν(C–C)	1313(w)	1309(w)
ν(C–C)	1434(w)	
ν(C–C)	1602(vs)	1602(vs)
ν(C═O)		1695(s)
ν(C–H)	3067(w)	3075(w)

ν, stretching; β, in-plane bending; γ, out-of-plane bending; vs, very strong; s, strong; m, medium; w, weak; vw, very weak.

Solid-state polymorphic transition of PABA determined by *in situ* Raman analyzer

As revealed by DSC, the β-form of PABA undergoes a solid–solid transition to the α-form on heating before melting. In order to get more information about the solid-state transition, kinetic studies were performed under isothermal conditions using the experimental setup as described above. The β-form crystals were present on the hot stage and held isothermally at different temperatures. The Raman spectra of the sample were collected *in situ* during phase transition experiments. A typical Raman waterfall plots during the transition in the region of

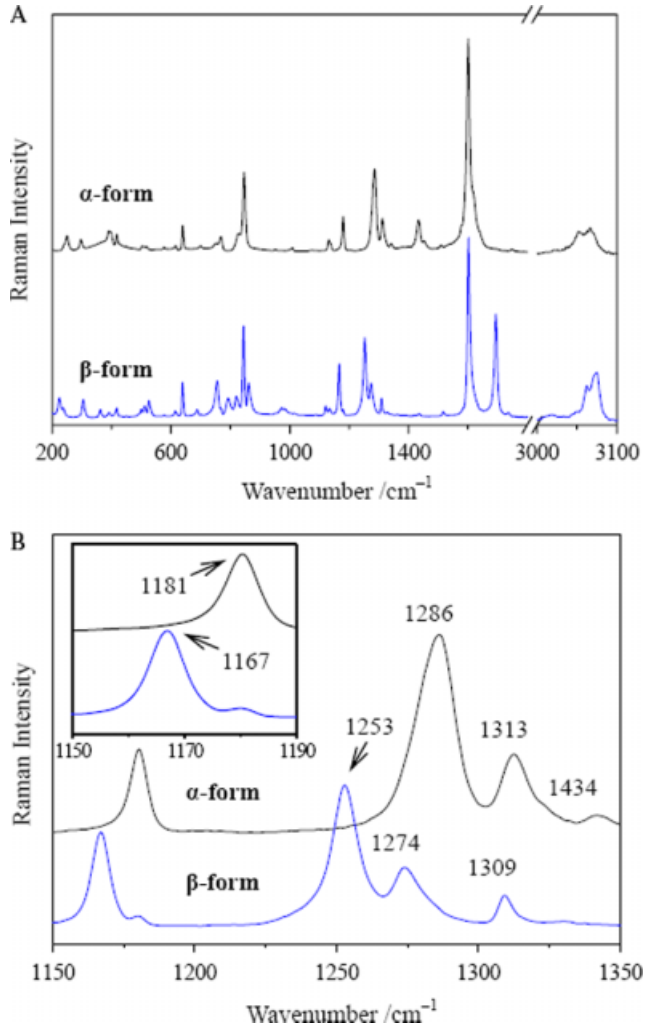

Figure 4. Raman spectra of solid-state α-form and β-form of PABA: (A) 200–3100 cm^{-1}; (B) highlighted region of 1150–1350 cm^{-1}. This figure is available in colour online at www.interscience.wiley.com/journal/jrs.

1150–1350 cm^{-1} are illustrated in Fig. 5(A). It shows the time course of the transition from β-form to α-form at 96 °C. As the transition proceeds, the characteristic peaks of the β-form are decreasing in intensity while those of the α-form appear and increase in intensity.

From Fig. 5(B), the Raman spectra changes between 1150 and 1190 cm^{-1} can be clearly observed. The figure shows the appearance, disappearance and change in intensity of the Raman characteristic peaks for each form. The Raman spectra between 1150 and 1190 cm^{-1} were used to monitor the progress of the transition. The normalized spectra changes in the region of 1150 and 1190 cm^{-1} during the transition process were computed by HoloReact software, which used the baseline-integrated areas to do calculations. The pure Raman spectra were normalized to a particular band of an internal standard. Figure 5(C) shows the transition trends of the two forms presented in arbitrary units. The green and blue curves represent the time profiles of the relative changes in the second derivative peak areas of α-form and β-form, respectively. As revealed by Raman waterfall plot, only two species (α-form and β-form) exist in the course of the transition, and the initial and final materials are pure β- and α-forms. A semi-quantitative analysis could now be employed to convert the original Raman response to mass fraction transformed. That means the data in Fig. 5(C) were rescaled between 0 and 100%.

Table 2. Kinetic equations and mechanisms of solid-state reactions

Model	Equation, $f(\alpha) = kt$	Mechanism
M1	$[-\ln(1-\alpha)]^{1/2}$	Avrami–Erofeev, $n = 2$
M2	$[-\ln(1-\alpha)]^{1/3}$	Avrami–Erofeev, $n = 3$
M3	$[-\ln(1-\alpha)]^{1/4}$	Avrami–Erofeev, $n = 4$
M4	α^2	One-dimensional diffusion
M5	$(1-\alpha)\ln(1-\alpha)+\alpha$	Two-dimensional diffusion
M6	$[1-(1-\alpha)^{1/3}]^2$	Three-dimensional diffusion (Jander)
M7	$1-2\alpha/3-(1-\alpha)^{2/3}$	Three-dimensional diffusion (Ginstling–Brounshtein)
M8	$\ln[\alpha/(1-\alpha)]$	Random nucleation (Prout–Tompkins)
M9	$-\ln(1-\alpha)$	First-order reaction
M10	$1/(1-\alpha)-1$	Second-order reaction
M11	α	One-dimensional phase boundary reaction
M12	$1-(1-\alpha)^{1/2}$	Two-dimensional phase boundary reaction
M13	$1-(1-\alpha)^{1/3}$	Three-dimensional phase boundary reaction

α: Mass fraction of α-form, $\alpha = 0.05$–0.95.

Figure 6 presents the rescaled transition profiles from isothermal experiments at six different temperatures: 78, 82, 86, 90, 96, and 100 °C. It can be seen that all the transition curves exhibit a sigmoidal shape: (1) an initial period of induction, defined as the time required to detect a considerable increase in conversion, (2) an acceleratory period of rapid increase in conversion which is corresponding to the accelerated three-dimensional growth of crystals, and (3) a decay period indicating the completion of the crystallization process. The time required to complete the transition decreases with increasing isothermal temperature, being of *ca* 115, 56, 30, 18, 11, and 5 min at 78, 82, 86, 90, 96, and 100 °C, respectively. In order to kinetically determine the transition of β-form to α-form, various solid-state reaction kinetic models[28–32] have been employed to derive the transition rate (Table 2). By fitting the experiment data in the range of 5–95 wt% fraction transformed to the equations $f(\alpha)$, a linear relation is predicted between $f(\alpha)$ and transition time t, and the corresponding slope gives the transition rate constant (k) at different temperatures. A correlation coefficient (R^2) analysis was performed for all the kinetic models and tabulated in Table 3. The results demonstrate that several models fairly fitted the data well, particularly for Avrami-Erofeev models (M1, M2, and M3) and Prout–Tompkins model (M8). The development of the Avrami–Erofeev relationship is based on the assumption that the solid phase transformation proceeds by a nucleation-and-growth mechanism.[33] The Prout–Tompkins model is based on branching nuclei with possible interference occurring between these nuclei.[34] This kinetic model has been commonly adapted to nucleation-rate-limited solid-state transformations. These analyses imply that the nucleation and growth of α-form within α- and β-form phase boundaries may play an important role in PABA polymorphic transition process.

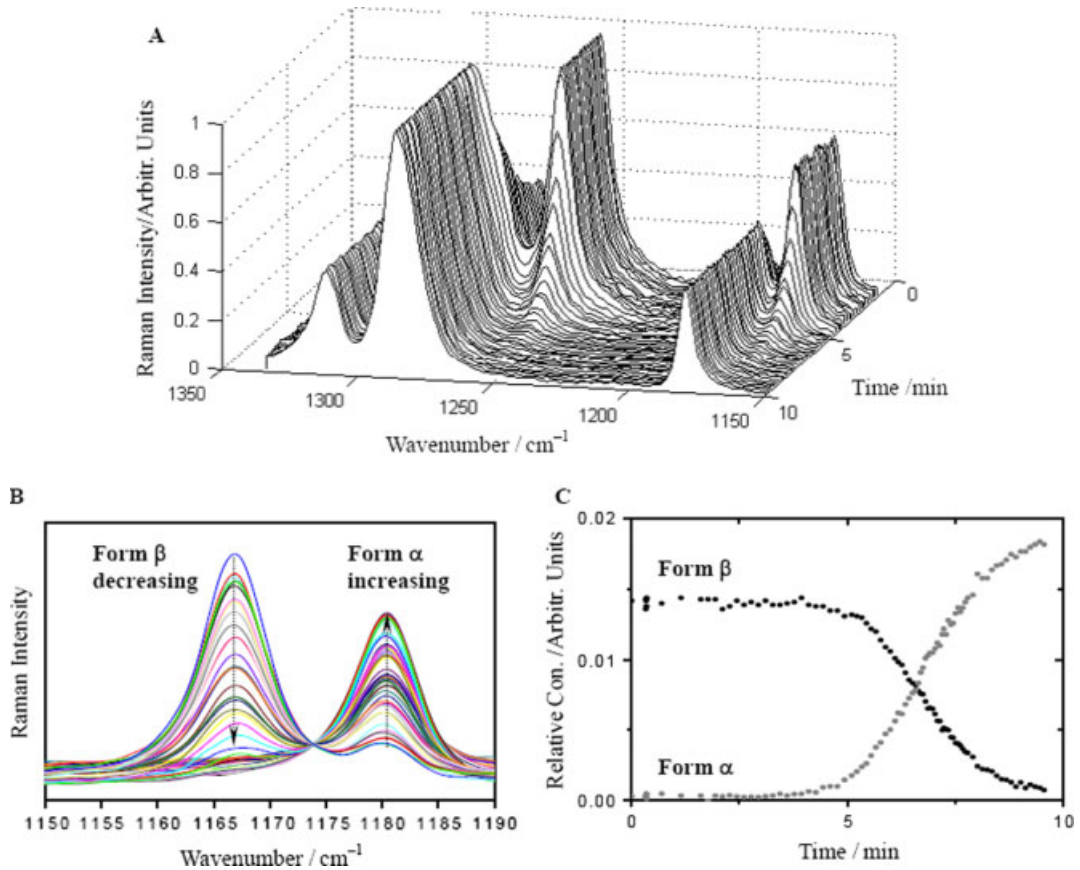

Figure 5. Solid-state transition from β-form to α-form at 96 °C: (A) real-time waterfall plots in the region of 1150–1350 cm^{-1}; (B) selected spectra; (C) corresponding transition trends presented in arbitrary units. This figure is available in colour online at www.interscience.wiley.com/journal/jrs.

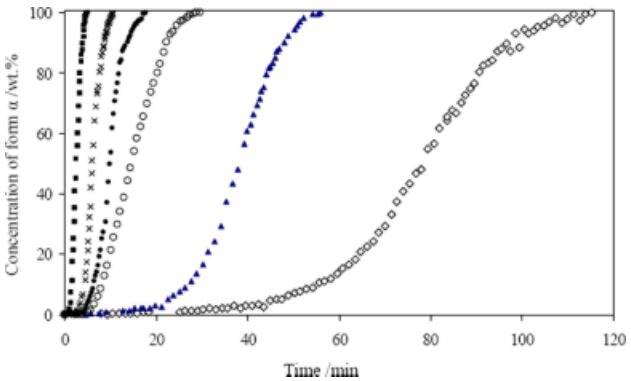

Figure 6. Contents of the α-form against time at different temperatures: (◊) 78 °C; (▲) 82 °C; (○) 86 °C; (●) 90 °C; (×) 96 °C; (■) 100 °C. This figure is available in colour online at www.interscience.wiley.com/journal/jrs.

Table 3. Correlation coefficients (R^2) for different kinetic models

Model	Correlation coefficient, R^2					
	78 (°C)	82 (°C)	86 (°C)	90 (°C)	96 (°C)	100 (°C)
M1	0.968	0.978	0.994	0.989	0.996	0.999
M2	0.989	0.993	0.996	0.989	0.989	0.994
M3	0.994	0.997	0.992	0.985	0.981	0.987
M4	0.918	0.927	0.974	0.952	0.978	0.983
M5	0.871	0.883	0.935	0.940	0.970	0.959
M6	0.777	0.792	0.841	0.897	0.926	0.895
M7	0.843	0.856	0.908	0.930	0.959	0.945
M8	0.992	0.995	0.989	0.994	0.988	0.989
M9	0.874	0.891	0.923	0.951	0.970	0.960
M10	0.581	0.596	0.619	0.750	0.763	0.734
M11	0.979	0.982	0.992	0.962	0.965	0.984
M12	0.954	0.962	0.992	0.976	0.991	0.997
M13	0.934	0.945	0.978	0.974	0.990	0.991

The suitability of the models to describe the kinetic data was also evaluated by Arrhenius equation

$$k = A\exp(-\frac{E_a}{RT})$$

where E_a is activation energy, R is Boltzman constant, and T is absolute temperature. The k values determined from the kinetic models were fit to Arrhenius plots of the natural logarithm of rate constants (ln$k$) against corresponding reciprocal temperatures, as shown in Fig. 7. The transition rate constants clearly increased with the rise of temperature. The activation energy E_a can be determined from the slope of the fitted Arrhenius plot. The activation energy is related to the hindrance involved in the transition of form β to form α. Table 4 shows the activation energy and R^2 produced with models M1, M2, M3, and M8. All of these models provide similar correlation coefficient, R^2, around 0.99. The

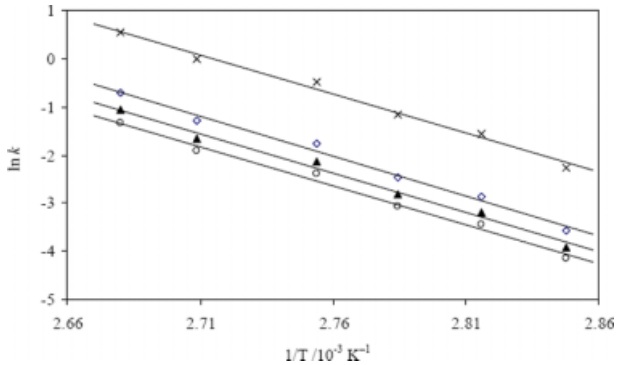

Figure 7. Arrhenius plots for the $\beta-\alpha$ transition of PABA using rate constants determined from the four kinetic models: (◊) M1 model; (▲) M2 model; (○) M3 model; (×) M8 model. This figure is available in colour online at www.interscience.wiley.com/journal/jrs.

Table 4. Calculated activation energies (E_a) for the transition using the four kinetic models

Model	Activation energy (kJ mol^{-1})	R^2	S_b
M1	137.7	0.991	0.052
M2	135.9	0.991	0.027
M3	134.7	0.990	0.016
M8	134.9	0.991	0.021

corresponding standard deviation of slope, S_b, is also reported. The average activation energy over the four models is 136.08 kJ mol^{-1}.

In addition, it has been found that the solid transition behavior is significantly affected by powder packing. In our experiments, the powder samples in compressed form generally show excellent repeatable results due to good thermal contact among solid particles. While the powder sample is with loose packing, heat transfer through the sample would be a key factor controlling the transition rate. To reduce heat transfer effects, the same amount of sample was compressed to disk with similar diameter and thickness before Raman analysis. It was found that no polymorphic transition of β-form crystals was observed during the compression.

Conclusions

The two different crystalline polymorphs of PABA (α- and β-forms) were identified and characterized by PXRD, TGA-DSC, and Raman spectroscopy. The solid-state transition from β-form to α-form has been probed using *in situ* Raman spectroscopy. It is shown that *in situ* Raman spectroscopy is a potentially powerful tool to monitor the polymorphic transition. The transition rate was expressed in terms of the fraction transformed as a function of time. For kinetic studies, the experimental data in the range of 0.05–0.95 fraction transformed were fitted to several solid-state reaction kinetic models. The best-fit model is chosen according to maximum correlation coefficient analysis. Of the various kinetic models considered, the Avrami–Erofeev and Prout–Tompkins models were found the best to correlate the experimental data.

References

[1] J. Bernstein, *Polymorphism in Molecular Crystals*, Clarendon Press: Oxford, **2002**.
[2] R. Hilfiker, *Polymorphism: In the Pharmaceutical Industry*, Wiley–VCH: Weinheim, **2006**.
[3] T. Mukuta, A. Y. Lee, T. Kawakami, A. S. Myerson, *Cryst. Growth Des.* **2005**, *5*, 1429.
[4] S. Jiang, J. H. ter Horst, P. J. Jansens, *Cryst. Growth Des.* **2008**, *8*, 37.
[5] D. Singh, P. V. Marshall, L. Shields, P. York, *J. Pharm. Sci.* **1998**, *87*, 655.
[6] A. K. Sheridan, J. Anwar, *Chem. Mater.* **1996**, *8*, 1042.
[7] M. Otsuka, M. Onoe, Y. Matsuda, *Pharm. Res.* **1993**, *10*, 577.
[8] C. Rustichelli, G. Gamberini, V. Ferioli, M. C. Gamberini, R. Ficarra, S. Tommasini, *J. Pharm. Biomed. Anal.* **2000**, *23*, 41.
[9] X. Yang, J. Lu, X. J. Wang, C. B. Ching, *J. Cryst. Growth.* **2008**, *310*, 604.
[10] A. P. Ayala, H. W. Siesler, S. L. Cuffini, *J. Raman Spectrosc.* **2008**, *39*, 1150.
[11] F. Wang, J. A. Wachter, F. J. Antosz, K. A. Berglund, *Org. Process Res. Dev.* **2000**, *4*, 391.
[12] T. Ono, J. H. ter Horst, P. J. Jansens, *Cryst. Growth Des.* **2004**, *4*, 465.
[13] J. Schöll, D. Bonalumi, L. Vicum, M. Mazzotti, *Cryst. Growth Des.* **2006**, *6*, 881.
[14] X. Yang, J. Lu, X. J. Wang, C. B. Ching, *J. Raman Spectrosc.* **2008**, *39*, 1433.
[15] L. E. O'Brien, P. Timmins, A. C. Williams, P. York, *J. Pharm. Sci.* **2004**, *36*, 335.
[16] H. Qu, M. Louhi-Kultanen, J. Rantanen, J. Kallas, *Cryst. Growth Des.* **2006**, *6*, 2053.
[17] Y. Hu, J. K. Liang, A. S. Myerson, L. S. Taylor, *Ind. Eng. Chem. Res.* **2005**, *44*, 1233.
[18] B. O'Sullivan, P. Barrett, G. Hsiao, A. Carr, B. Glennon, *Org. Process Res. Dev.* **2003**, *7*, 977.
[19] J. Aaltonen, P. Heinänen, L. Peltonen, H. Kortejärvi, V. P. Tanninen, L. Christiansen, J. Hirvonen, J. Yliruusi, J. Rantanen, *J. Pharm. Sci.* **2006**, *95*, 2730.
[20] G. N. R. Tripathi, Y. Su, *J. Am. Chem. Soc.* **1996**, *118*, 2235.
[21] C. F. Chignell, B. Kalyanaraman, R. P. Mason, R. H. Sik, *Photochem. Photobiol.* **1980**, *32*, 565.
[22] T. F. Lai, R. E. Marsh, *Acta Crystallogr.* **1967**, *22*, 885.
[23] S. Gracin, A. Fischer, *Acta Crystallogr.* **2005**, *E61*, o1242.
[24] S. Gracin, A. C. Rasmuson, *Cryst. Growth Des.* **2004**, *4*, 1013.
[25] R. Świsłocka, M. Samsonowicz, E. Regulska, W. Lewandowski, *J. Mol. Struct.* **2006**, *792–793*, 227.
[26] M. Samsonowicz, T. Hrynaszkiewicz, R. Świsłocka, E. Regulska, W. Lewandowski, *J. Mol. Struct.* **2005**, *744–747*, 345.
[27] N. Sundaraganesan, S. Ilakiamani, B. Dominic Joshua, *Spectrochim. Acta, Part A* **2007**, *67*, 287.
[28] W. E. Garner, *Chemistry of the Solid State*, Academic Press: New York, **1955**.
[29] M. Avrami, *J. Chem. Phys.* **1939**, *7*, 1103.
[30] B. V. C. R. Erofeyev, *(Dokl.) Acad. Sci. URSS.* **1946**, *52*, 511.
[31] E. G. Prout, F. C. Tompkins, *Trans. Faraday Soc.* **1944**, *40*, 488.
[32] S. R. Byrn, R. R. Pfeiffer, J. G. Stowell, *Solid-State Chemistry of Drugs* (2nd edn), SSCI, Inc.: West Lafayette, IN, **1999**.
[33] H. Zhu, D. J. W. Grant, *Int. J. Pharm.* **2001**, *215*, 251.
[34] U. M. Gundusharma, E. A. Secco, *Solid State Ionics* **1990**, *44*, 47.